

Targeted Co-delivery of PTX and TR3 siRNA by PTP Peptide Modified Dendrimer for the Treatment of Pancreatic Cancer

Yang Li, Hebin Wang, Kai Wang, Qinglian Hu, Qi Yao, Youqing Shen, Guocan Yu,* and Guping Tang*

Pancreatic cancer is the fourth leading cause of cancer deaths and shows a rapid clinical course with a 5-year survival rate of less than 5%, becoming a major health issue and a great clinical challenge in the coming years.^[1–3] The incidence and the mortality of pancreatic cancer increase dramatically over the past decades.^[4] Recently, some progress has been made in the diagnosis and treatment of pancreatic cancer. Several chemotherapy agents, including gemcitabine (GEM), paclitaxel (PTX), and 5-fluorouracil, show moderate efficacy in the treatment of pancreatic cancer,^[5,6] whereas negligible survival benefit is achieved. Development of new therapeutic means is urgently needed for the vast majority of pancreatic patients. Recently, combination therapy is widely utilized to cooperatively inhibit the proliferation of tumor cells with combined effects through different antitumor mechanisms.^[7–9] For example, Zhu and co-workers developed the

amphiphilic drug–drug conjugate for cancer therapy, which exhibited excellent anticancer activity in vitro and in vivo.^[10] Hao and co-workers confirmed that a combination of three chemotherapy agents (5-fluorouracil, irinotecan, oxaliplatin) proved to be efficient for pancreatic cancer therapy.^[11] However, chemotherapy also faces several limitations, including fast blood/renal clearance, poor bioavailability, and multi-drug resistance.^[12] Furthermore, the shortage of targeting selectivity leads to serious side effects toward normal tissues, greatly limiting their efficacy and clinic applications.

Due to its high specificity and low toxicity,^[13,14] small interfering RNA (siRNA) is able to silence almost any target gene after cellular delivery, providing them with great potential for gene therapy for various diseases, including cancer.^[15,16] A variety of siRNA-based therapeutics have been developed, showing great promise in cancer treatments.^[17–19] Orphan nuclear receptor TR3/Nur77 is a new therapeutic target for pancreatic cancer therapy, which is reported overexpressed in a panel of human pancreatic tumors (77%), the endogenous TR3 not only facilitates cell growth but also cell survival by repressing apoptosis.^[20,21] siTR3 decreases TR3 mRNA and TR3/Nur77 protein, and this is accompanied by decreasing expression of Bcl-2 and Survivin and induction of cleaved caspase-3 and poly ADP ribose polymerase (PARP) cleavage, confirming the activation of apoptosis.^[22,23] As a result, knocking down TR3 signal pathway is potential to prevent the proliferation of pancreatic cancer. Tumorigenesis involves multiple mechanisms that enable cancer cells to sustain proliferative signaling, resist cell death and induce angiogenesis, which makes cancer treatment extremely challenging. Currently, co-delivery of siRNA and chemotherapeutic drugs to tumor cells is a vital means to silence target genes and overcome the side effects of the chemotherapy for an improved chemotherapeutic effect.^[24]

However, it remains a challenge to design sophisticated nanocarriers with the capability to co-delivery of siRNA and chemotherapeutic drugs because of the different physicochemical properties of each part.^[25] Naked siRNA hardly penetrates across cell membranes due to their high-molecular-weight and high density of negative charge.^[26] Moreover, it is easily degraded by nucleases in plasma, resulting in the inactivation of the siRNA.^[27] For general chemotherapeutic drugs, such as PTX, doxorubicin, GEM, the solubility and stability are always poor in physiological environment.

Y. Li, H. Wang, Dr. K. Wang, Q. Yao, Prof. G. Tang
Institute of Chemical Biology and Pharmaceutical
Chemistry
Department of Chemistry
Zhejiang University
Hangzhou 310028, China
E-mail: tangguping@zju.edu.cn



H. Wang
College of Life Sciences
Tarim University
Alar 843300, China
Prof. Dr. Q. Hu
College of Biotechnology and Bioengineering
Zhejiang University of Technology
Hangzhou 310032, China

Prof. Y. Shen
Center for Bionanoengineering and State Key Laboratory
for Chemical Engineering
Department of Chemical and Biological Engineering
Zhejiang University
Hangzhou 310027, China

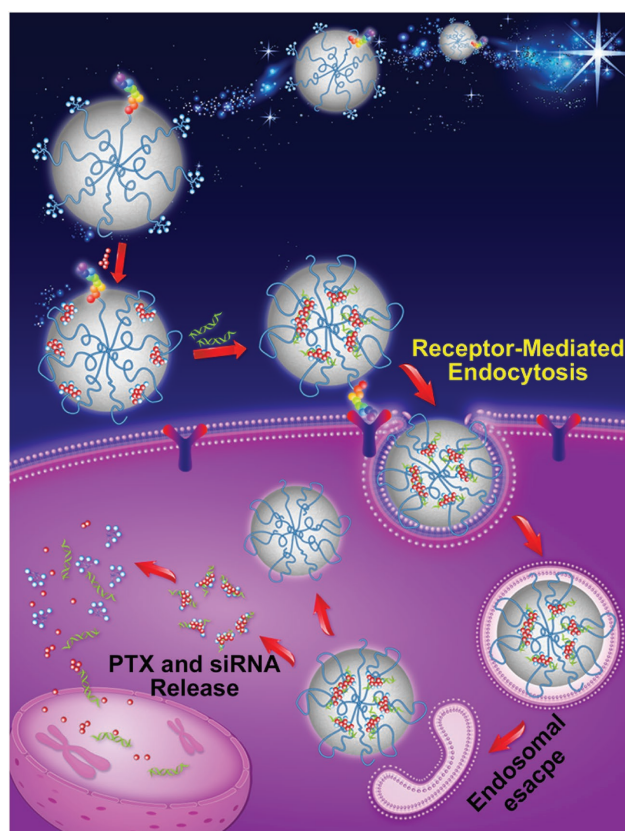
Dr. G. Yu
Laboratory of Molecular Imaging and Nanomedicine (LOMIN)
National Institute of Biomedical Imaging and Bioengineering (NIBIB)
National Institutes of Health (NIH)
Bethesda, MD 20892, USA
E-mail: guocan.yu@nih.gov

DOI: 10.1002/sml.201602697

To overcome these issues, researchers have specially developed various systems by using polymeric micelles,^[28,29] liposomes^[30] and silica-based nanomaterials,^[31,32] dendrimers,^[33] and other organic/inorganic hybrid materials.^[34] Among them, polymeric nanoparticles (NPs) exhibit unparalleled advantages as nanovehicles due to their excellent biocompatibility and easy functionalization.^[35,36] Dendrimers are a popular class of materials for drug and gene therapy due to their unique highly branched and highly precise molecular structure to meet specific needs in different situation.^[37,38] We previously developed a redox-sensitive co-delivery system based on branched poly(ethylene glycol) with G2 dendrimers through disulfide linkages (**PSPG**), responsive to the intracellular glutathione (GSH) to release the hydrophobic drugs and siRNA.^[39] The co-delivery NPs exhibit dynamic and structure-invertible properties, which are effective to simultaneously deliver nucleic acids and hydrophobic drugs for combination cancer therapy. However, this system showed limited accumulation in vivo and lacked the tumor-targeted for cancer therapy.

Herein, PTP (plectin-1 targeted peptide, NH₂-KTLPTP-COOH), a novel biomarker of pancreatic cancer,^[40] is coupled with the **PSPG** vector to form peptide-conjugated **PSPG** (**PSPGP**) nanoparticles for targeted co-delivery of nuclear receptor siRNA (siTR3) and hydrophobic drug (PTX) in vitro and in vivo. The PTP targeted NPs specifically accumulate in cancer cells through receptor-mediated cell endocytosis. Once entering into cells, the loaded siRNA and PTX released from the NPs to exert their therapeutic functions due to the cleavage of disulfide linkages in the intracellular glutathione-rich reduction environment. In vitro studies indicate that the **PSPGP**/PTX/siTR3 ternary system effectively facilitates cellular uptake and exhibits high gene transfection in Panc-1 cell lines. siTR3 mediated knockdown of TR3 decreases the expression of antiapoptotic proteins, including Bcl-2 and Survivin in pancreatic cancer cells. For systemic in vivo delivery, the functional co-delivery system is expected to extensively accumulate in tumor tissue, significantly inhibiting tumor growth and inducing cancer cell apoptosis. Moreover, co-delivery of siTR3 and PTX reveals a synergetic effect to inhibit cancer cell growth in murine tumor models in vivo, which is much more efficient than either siTR3- or PTX-based monotherapy. Such PTP peptide-conjugated siTR3 and PTX co-delivery NPs have great potential applications in pancreatic cancer therapy.

In this study, PTP peptide-conjugated **PSPG** nanoparticles (**PSPGP**) possessing redox-sensitivity were successfully synthesized for co-delivery of PTX and siTR3. Intracellular delivery process of **PSPGP**/PTX/siTR3 ternary complex indicated that **PSPGP** exhibited enhanced endosomal escape and reduced intracellular degradation that facilitated efficient PTX and siRNA release in the cytosol (**Scheme 1**). **PSPGP** was prepared by conjugating branched poly(ethylene glycol) with dendrimers of two generations (G2) through disulfide linkages. **PSPGP** was synthesized according to the reported literature.^[39] Briefly, PTP was added to the solution of propargylamine (CC) was activated by *N*-succinimidyl-3-(2-pyridyldithiol) propionate to afford **CC-SS-PTP**. Then, click reaction was conducted by mixing **PSPG**/N₃ and **CC-SS-PTP**



Scheme 1. Schematic illustration of PTX-loaded, TR3 siRNA complexed co-delivery vectors and their structure inversion after nucleic acid complexation. Intracellular delivery process of **PSPGP**/PTX/siTR3 ternary complexes indicates that **PSPGP** exhibited enhanced endosomal escape and intracellular degradation that facilitates efficient PTX and siRNA release in the cytosol.

in the presence of CuSO₄ (5 mol%) and sodium ascorbate (10 mol%). The successful preparation of **PSPGP** was confirmed by proton nuclear magnetic resonance (¹H NMR) spectroscopy (**Figure 1**). The existence of disulfide bonds was confirmed by the observation of the signals at 2.7–2.9 ppm corresponding to the protons on cystamine moiety. Furthermore,

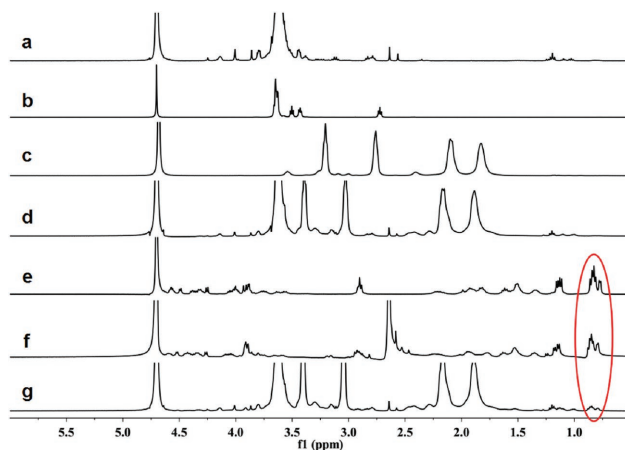


Figure 1. ¹H NMR spectrum (400 MHz, room temperature, D₂O) of a) **PSP**, b) N₃-PEG-NH₂, c) G2 Dendrimer, d) **PSPG**/N₃, e) **PTP**, f) **CC-SS-PTP** and g) **PSPGP**.

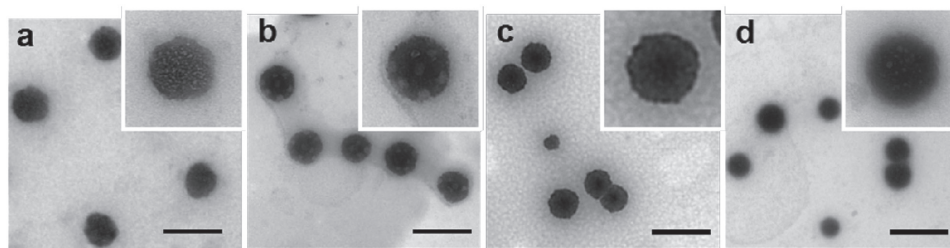


Figure 2. TEM images of a) **PSPGP**, b) **PSPGP/siRNA**, c) **PSPGP/PTX**, and d) **PSPGP/PTX/siRNA** complexes. The scale bars represent 500 nm.

characteristic resonances related to the protons on PTP appeared in the ^1H NMR spectrum ranging from 0.3 to 1.5 ppm, verifying the synthesis of **PSPGP** (Figure 1).

The size and morphology of the **PSPGP**, **PSPGP/PTX**, **PSPGP/siRNA**, and **PSPGP/PTX/siRNA** complexes were characterized by transmission electron microscopy (TEM) and atomic force microscope. As shown in **Figure 2** and Figure S2 (Supporting Information), the spherical structures were observed ≈ 200 nm in diameter. The suitable size and positive charge of the NPs were prerequisites to effective cellular internalization. As shown in **Figure 3**, the average diameter of these NPs was calculated to be around 200 nm and the zeta potential of the NPs stabilized at low values in the range of 1–6 mV accompanied with the increase of the N/P ratios (Figure 3a,b). This phenomenon was attributed to the existence of neutral poly(ethylene glycol) (PEG) shell that sheltered the surface charge of cationic **PSPGP** polyplexes after the structure inversion.^[39,41,42] The NPs with suitable size were favorable for passive targeting tumor though

the enhanced permeability and retention (EPR) effect^[43,44] and positive surface potential increased the endocytosis by increasing the interaction with the cell membrane.^[44,45] To measure the PTX-loading capacity of **PSPGP/PTX/siTR3**, drug-loading content was measured depending on different feed ratios of PTX to **PSPGP/PTX/siTR3** shown in Figure 3c. PTX was efficiently entrapped in a wide range of feed weight ratios, and the drug loading content ranged from 4.63 to 13.9 wt%. This result indicated that the PTX loading content in **PSPGP/PTX/siTR3** was adjustable, which was an important peculiarity for codelivery systems.

The property of drug release from the co-delivery system is very important for anti-tumor efficacy in intracellular environment.^[46] The most attractive function of **PSPGP/PTX/siTR3** was their ability to quickly release PTX and siRNA in physiological reducing environment. Due to the breakage of disulfide bonds, the imbedded cationic dendrimers separated from 8-armed PEG backbone, resulting in the release of the loaded PTX and siTR3. To investigate the redox-triggered

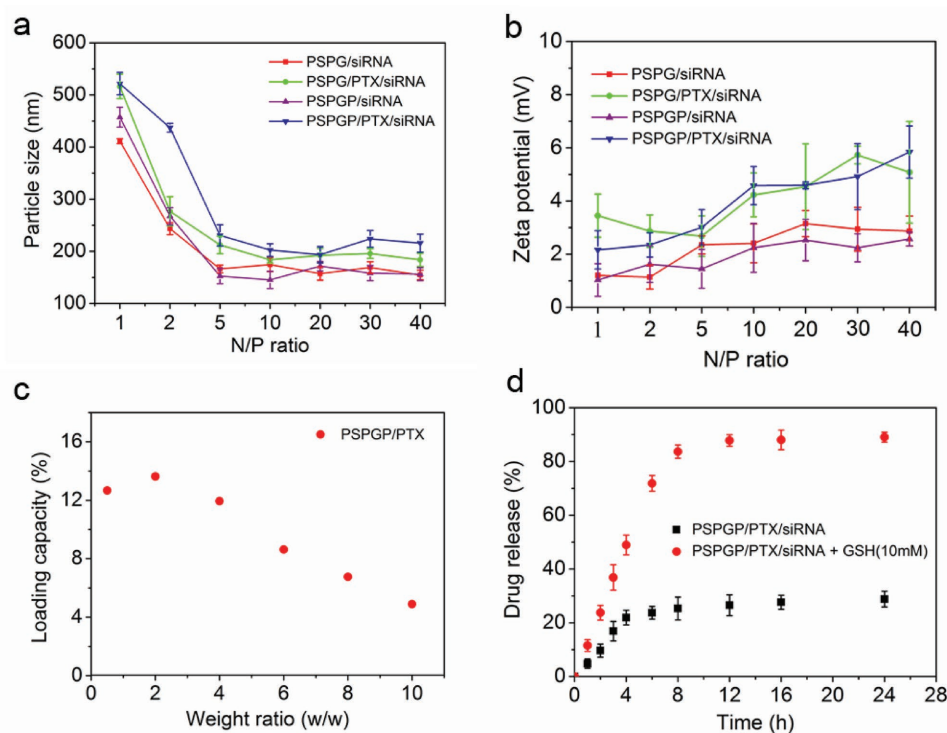


Figure 3. a) The particle size and b) zeta potential of **PSPG/siRNA**, **PSPG/PTX/siRNA**, **PSPGP/siRNA**, and **PSPGP/PTX/siRNA** complexes at different N/P ratio (pH 7.4). c) The PTX loading capacity of **PSPGP** and PTX as a function of initial feed ratio of **PSPGP/PTX**. d) Time-dependent release of PTX from **PSPGP/PTX/siRNA** complexes in the presence or absence of 10×10^{-3} M GSH.

drug release behavior, the ternary NPs were incubated in phosphate buffer (PBS, pH 7.4) in the absence and presence of 10×10^{-3} M intracellular GSH to simulate the normal extracellular environment and the intracellular circumstance. As shown in Figure 3d, about 20% of PTX was released from **PSPGP**/PTX/siTR3 NPs over 12 h in the absence of GSH. Whereas, a rapid release of PTX was monitored in the presence of GSH, and about 80% of PTX was sustained release from **PSPGP**/PTX/siTR3 NPs over 12 h. These results suggested that the **PSPGP** NPs maintained excellent stability in the normal extracellular environment and may efficiently release PTX and siRNA at cytosol where GSH was rich.

The ability of the **PSPGP** to deliver siRNA and induce gene silencing was investigated using 293T/GFP cells that stably expressed the green fluorescent protein (GFP). The gene silencing ability of **PSPGP**/PTX/siRNA became optimal at N/P ratio of 10, showing up to 35% of GFP knockdown (Figure 4d). These results demonstrated that **PSPGP** mediated efficient siRNA-based gene silencing. For the co-delivery system, the internalization of the siRNA and drug into cells was the prerequisite for its pharmacological effect.^[47] To explore the cellular uptake and release of cargos from the NPs, **PSPGP**/PTX/FAM-siRNA complexes were visualized in Panc-1 cells using confocal laser scanning microscopy (CLSM). As shown in Figure 4c, green fluorescence was observed mainly in the cytoplasm for all experimental time points, suggesting that the NPs were able to co-delivery of the siRNA and drug efficiently and release the cargos in the cytosol where GSH was rich. In our previous study, **PSPGP**

showed excellent biocompatibility both in vitro and in vivo. After PTP was grafted, the cytotoxicity of the NPs was identical or even slightly lower than that of **PSPG**. To assess the synergistic anticancer effect of the co-delivery system, cytotoxicity against Panc-1 cells and HeLa cells was evaluated by MTT assay. The cells were incubated with a series of doses of free PTX, siTR3, PTX-loaded, and siTR3-loaded NPs for 24 h. Dose-dependent cytotoxicity of these NPs was observed, along with the changes of PTX and siTR3 concentration. Increasing the concentration of PTX or PTX-loaded NPs reduced the cell viability (Figure 4a). Compared with free PTX, PTX-loaded NPs exhibited higher toxicity in the range of experimental concentrations. The cytotoxicity of the free siTR3 was ignored, whereas siTR3-loaded NPs exhibited high toxicity (Figure 4b). In the case of **PSPGP**/PTX/siTR3, the ternary NPs display the highest toxicity in the given dose, confirming the synergistic effect in this system. As shown in Figure 4a,b, the NPs containing the targeting peptide showed higher cytotoxicity toward Panc-1 cells than those of the **PSPG** systems without targeting PTP peptide. It should be noted that the negligible difference in cytotoxicity toward HeLa cells (Figure S3, Supporting Information) was observed for the NPs with and without targeting PTP peptide. These investigations strongly demonstrated that the PTP peptide on the surface of the vehicles acted as targeting groups, resulting in the specific delivery of the loaded drug/siRNA to Panc-1 cells.

In order to investigate the knockdown level of siTR3 in vitro, immunofluorescence assay was carried out. As shown in Figure 5 and Figure S4 (Supporting Information), when

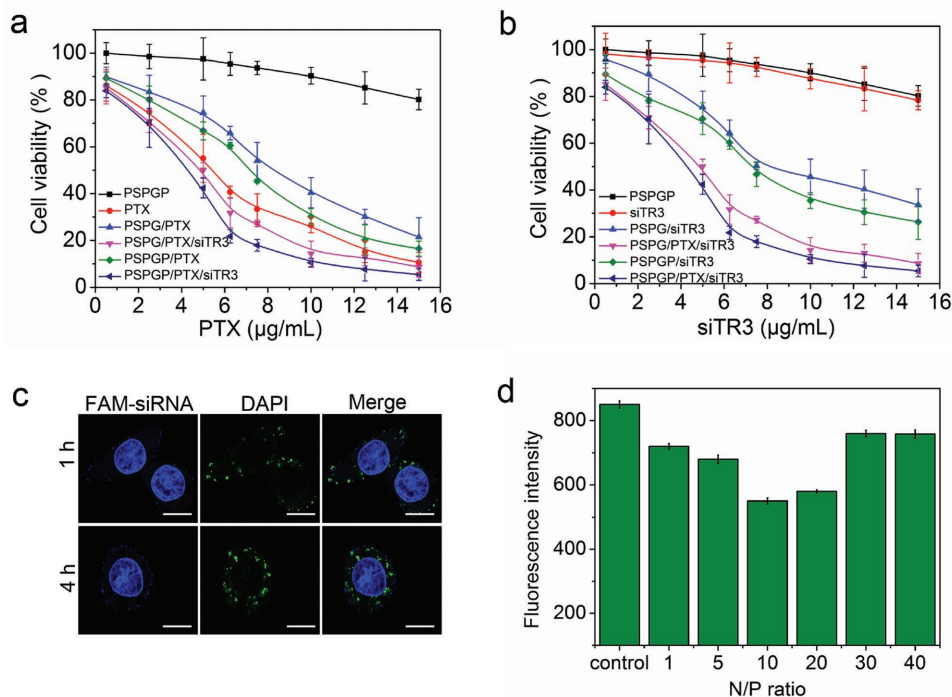


Figure 4. a,b) MTT assay toward Panc-1. The cells were treated with the complexes at different concentration for 24 h. c) Time-dependent in vitro CLSM images of Panc-1 cells transfected with **PSPGP**/PTX/FAM-siRNA. The scale bar represents 20 μm. d) The GFP knockdown 48 h after transfection with **PSPGP**/PTX/GFP-siRNA complexes at different N/P ratios in 293T/GFP cells. Control denotes to the fluorescence obtained from the cells without the treatment of siRNA polyplexes. Data represent mean ± SD ($n = 3$, Student's *t*-test, $*P < 0.05$).

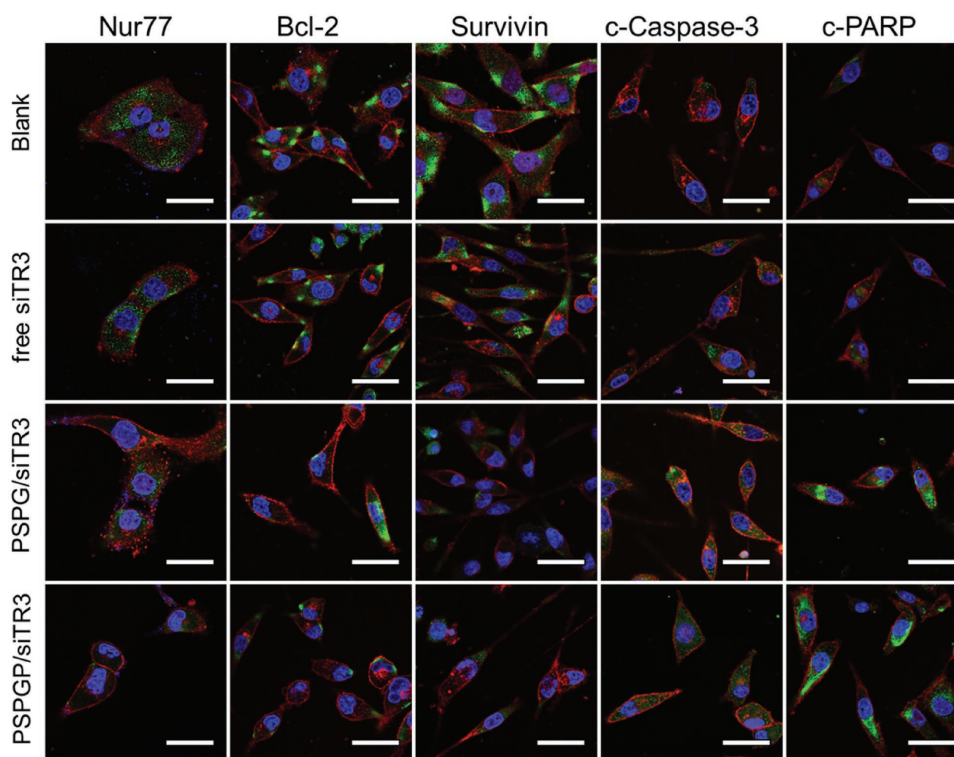


Figure 5. In vitro immunofluorescence image of Panc-1 cells transfected with free siTR3, **PSPG**/siTR3, and **PSPGP**/siTR3 at 24 h. Nur77, Bcl-2, Survivin, c-Caspase, and c-PARP were labeled with the corresponding antibody, and the secondary antibody (green) was Alexa Fluor 488 goat anti-rabbit IgG (H+L). Plasma membranes (red) were stained with Alexa Fluor 647 WGA and cell nuclei (blue) were stained with DAPI. Scale bars represent 20 μ m.

the Panc-1 cells were cultured with naked siTR3, **PSPG**/siTR3, **PSPGP**/siTR3, the expression of the Nur77, Bcl-2, and Survivin proteins were downregulated, which confirmed the decreased proliferation, induced apoptosis, and decreased expression of antiapoptotic genes. On the other hand, the proteins of the caspase-3 and PARP were upregulated, because Survivin was a member of the inhibitor of apoptosis protein family inhibiting apoptosis through interactions with caspases. A recent report showed that a Nur77-derived nanoparticle could be used to convert Bcl-2 into a proapoptotic moiety, which initiated apoptosis.^[48] One of the major targets of TR3 in pancreatic cancer cells was Survivin, which was overexpressed in pancreatic tumors and may be a drug target for cancer chemotherapy. As a consequence, activation of TR3/Nur77 promoted apoptosis and inhibited pancreatic tumor growth.^[21,22] Those results also confirmed that siTR3 decreased TR3 mRNA and Nur77 protein, and this was accompanied by decreased expression of Bcl-2 and Survivin and induction of cleaved caspase-3 and PARP cleavage. It should be pointed out that the **PSPGP**/siTR3 group effectively downregulated the level of the Nur77, Bcl-2, and Survivin protein, which was more effective than those of the **PSPG**/siTR3 and the naked siTR3 groups (Figure 5), emphasizing the targeting ability of PTP peptide.

In vivo fluorescence imaging experiments were carried out to demonstrate the targeting ability of **PSPGP**/PTX/siTR3, the nude mice bearing Panc-1 tumor were administered by **PSPGP**/Rho-PTX/FAM-siRNA, **PSPG**/Rho-PTX/FAM-siRNA, Rho-PTX/FAM-siRNA or PBS via intravenous

(i.v.) injections. Fluorescent images of mice were acquired at different time intervals. The fluorescence intensities of Rho and FAM were detected through their individual channels (**Figure 6**). Because naked siRNA was rapidly degraded and lacked the targeted ability, no obvious fluorescence signals in tumor and organs were detected for the free Rho-PTX/FAM-siRNA group. Notably, the mice formulated with **PSPGP**/Rho-PTX/FAM-siRNA showed high fluorescent signal at tumor site. The intensity of the signal sustained from 4 to 24 h, indicating that the ternary NPs well accumulated in tumors, due to the combination of EPR effect and the active targeting ability of PTP. These results indicated that **PSPGP**/Rho-PTX/FAM-siRNA co-delivery system preferentially accumulated at site of the tumor and had the high tumor targeting ability.

The mice were randomly assigned to seven groups and treated with the PBS, **PSPGP**, **PSPGP**/PTX, **PSPGP**/siTR3, **PSPG**/PTX/siTR3, **PSPGP**/PTX & **PSPGP**/siTR3, **PSPGP**/PTX/siTR3, respectively, to test the anti-tumor activity and systemic toxicity. The tumor volume and body weight were measured every 3 d up to 42 d. As shown in **Figure 7a**, rapid tumor growth was observed for the mice treated with PBS. Compared with the groups treated with PBS or **PSPGP**, simultaneous delivery of PTX and siTR3 by **PSPGP** exhibited moderate inhibition of tumor growth. In contrast, delivery of separate siTR3 and PTX by **PSPGP** showed slight inhibition of tumor growth and no synergistic effect was observed, primarily due to the separate internalization of the two complexes. Excitingly, the tumor-targeted co-delivery

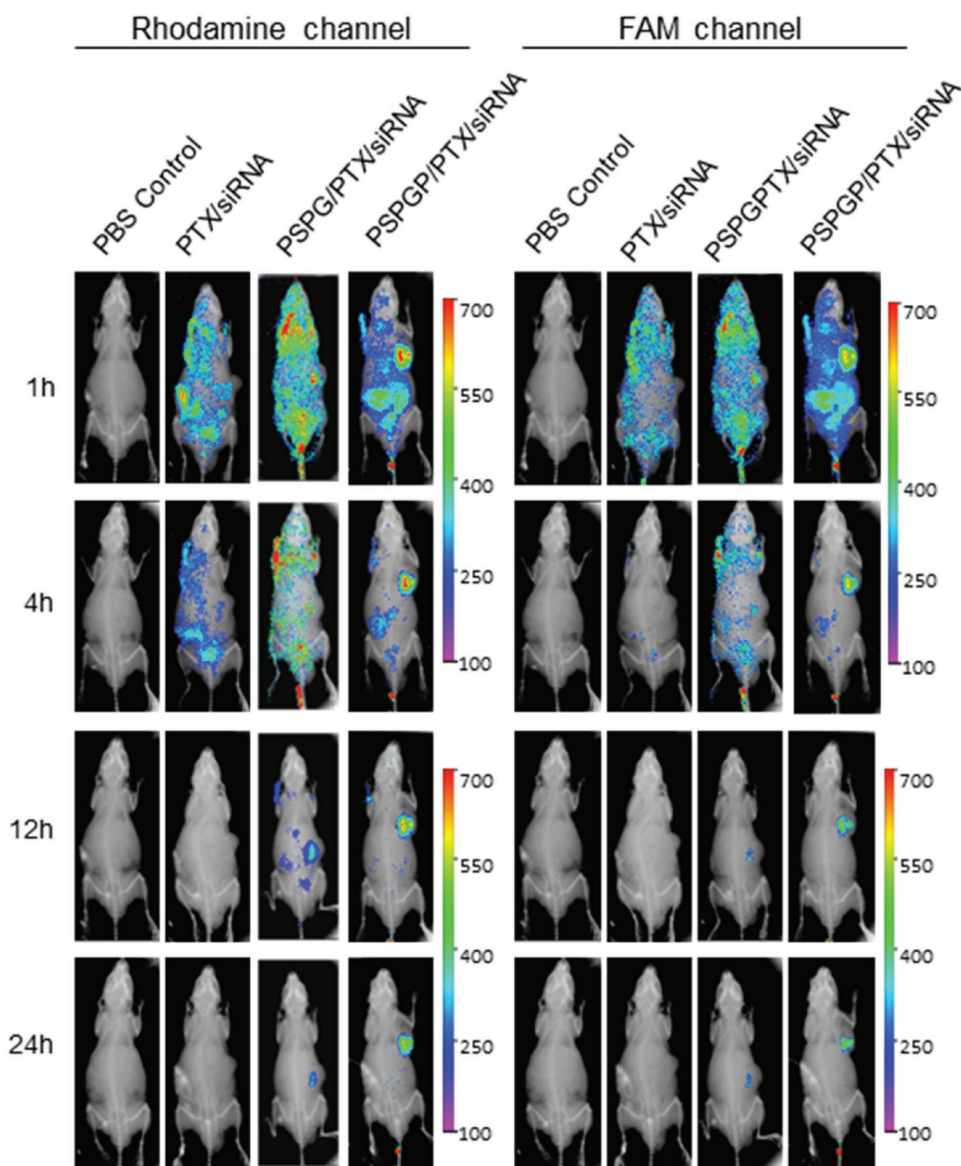


Figure 6. Fluorescence images of Panc-1 xenograft-bearing mice after intravenous injection of PBS, **PSPGP/PTX/siRNA**, **PSPG/PTX/siRNA**, and PTX/siRNA. PTX was labeled with rhodamine and siRNA was labeled with FAM.

system **PSPGP/PTX/siTR3** showed a more effective anti-tumor growth effect than the **PSPG/PTX/siTR3** group, which is attributed to the targeting function of PTP peptide. These results demonstrated that a strong synergistic effect in treating cancer could be obtained through co-delivery of PTX and siTR3. The positron emission tomography (PET) imaging was used to further confirm the anti-tumor efficacy of the different formulations (Figure 7c). It was apparently shown that the tumor size and intensity were decreased dramatically from left to right, verifying that the targeting codelivery system inhibited cancer progression effectively. No significant body weight loss was recorded in mice, indicating the favorable toxicity nature and minimal side effect of the **PSPGP/PTX/siTR3** NPs (Figure 7b). These results highlighted the significance of codelivery of siTR3 and PTX therapy for in vivo cancer treatment.

Cell proliferation and apoptosis in the tumors were analyzed by hematoxylin and eosin (H&E) staining, Ki67, and terminal deoxynucleotidyl transferase dUTP nick end labeling (TUNEL) assay after treatment (**Figure 8a**). The H&E stained sections of tumor tissues in PBS group appear most hypercellular and showed more obviously the nuclear polymorphism. Among the seven therapeutic groups, the tumor tissues from the treatment of **PSPGP/PTX/siTR3** NPs showed the fewest tumor cells and the highest level of tumor necrosis. The Ki67 assay indicated that co-delivery of PTX and siTR3 by the **PSPGP** NPs reduced the percentage of proliferating tumor cells and showed a particularly significant decrease of Ki67-positive tumor cell. As expected, TUNEL assay confirmed that treatment with **PSPGP/PTX/siTR3** resulted in significantly reduced proliferation and increased apoptosis compared that of the other groups, in

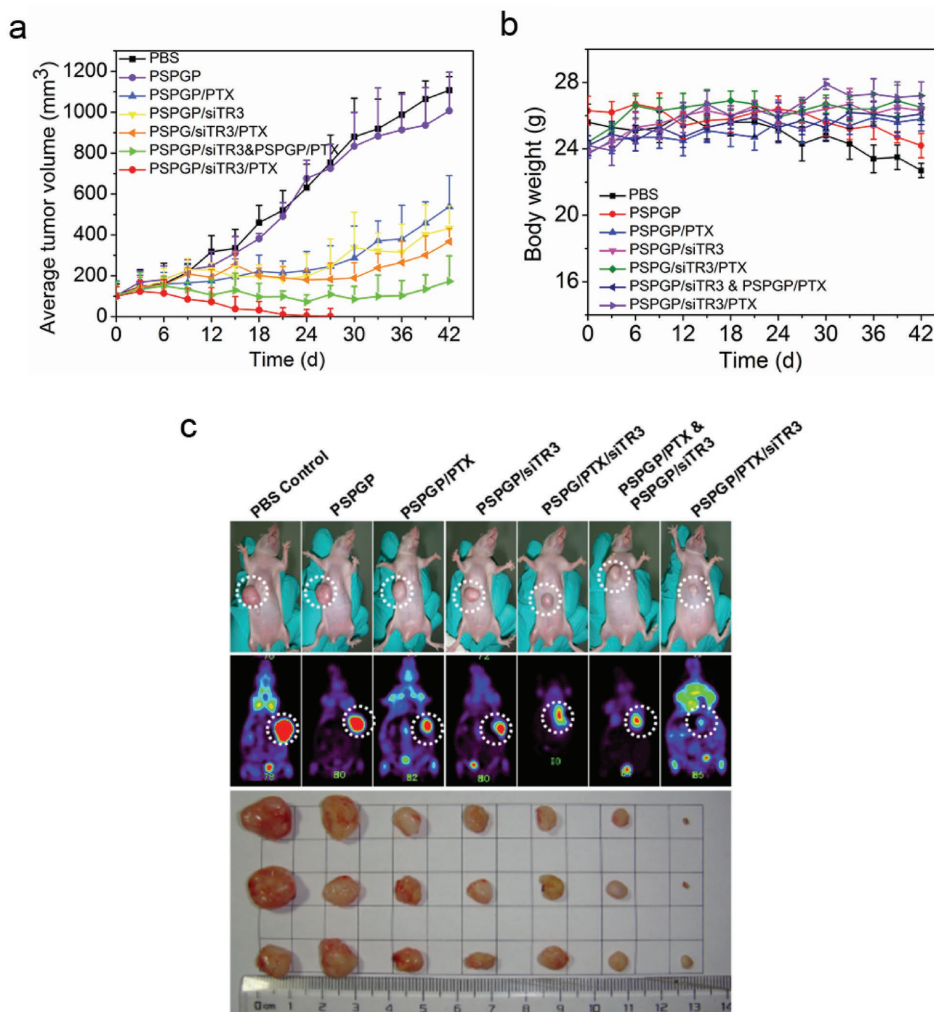


Figure 7. Murine tumor models with Panc-1 xenografts treated with PBS, **PSPGP**, **PSPGP/PTX**, **PSPGP/siTR3**, **PSPGP/PTX/siTR3**, **PSPGP/PTX & PSPGP/siTR3**, **PSPGP/PTX/siTR3**. a) Inhibition of tumor growth in murine tumor models 18 d after the first treatment and another 24 d (** $P < 0.01$). b) Average body weight of mice vaccinated with the different formulations in murine tumor model 18 d after the first treatment and another 24 d. c) PET images of in vivo tumor growth and photo-images of dissected tumor tissues 18 d after the first treatment, the intensity is shown by the legend to the right.

agreement with the results obtained from H&E and Ki67 analyses.

Immunohistochemical assays were further performed to detect the expression of five target proteins in tumor tissues of mice after different treatments. Analysis of tumor tissues, Nur77, Bcl-2, and Survivin proteins staining revealed a distinct decrease in the protein density of the tumor slice after the co-delivery of PTX and siTR3, when compared with the **PSPGP/PTX** & **PSPGP/siTR3** and other formulations, however, the cleaved caspase-3 and cleaved PARP proteins increased significantly as shown in Figure 8b. In vivo anti-tumor efficacy of co-delivery treatment suggested that co-delivery of PTX and TR3 siRNA exerted a synergistic effect against tumor growth in murine tumor models. The evidence also demonstrated that **PSPGP** played an important role as an efficient co-delivery system for the cancer treatment in vivo. The outcomes of immunohistochemical assays were in accord with the in vitro immunofluorescence.

In conclusion, we successfully synthesized a new type of tumor-targeted, redox-responsive nanovehicle **PSPGP** for effective co-delivery of PTX and nuclear receptor siTR3 to treat pancreatic cancer. **PSPGP** were composed with G2 dendrimer modified 8-armed PEG and the surface was functionalized with tumor targeting PTP peptide, which linked through redox-responsive disulfide bonds. The **PSPGP/PTX/siTR3** NPs exhibited excellent loading capacities for both siRNA and PTX with flexible mass ratio. In vitro study demonstrated that siTR3 mediated knockdown of TR3 meanwhile decreased the expression of antiapoptotic proteins including Bcl-2 and Survivin in pancreatic cancer cells. More importantly, the co-delivery system showed a synergistic effect both in vitro and in vivo. In vivo study also showed that the tumor-targeted co-delivery system could significantly inhibit tumor growth and induce cancer cell apoptosis. Therefore, simultaneous delivery of siTR3 and PTX by the tumor-targeted, redox-sensitive

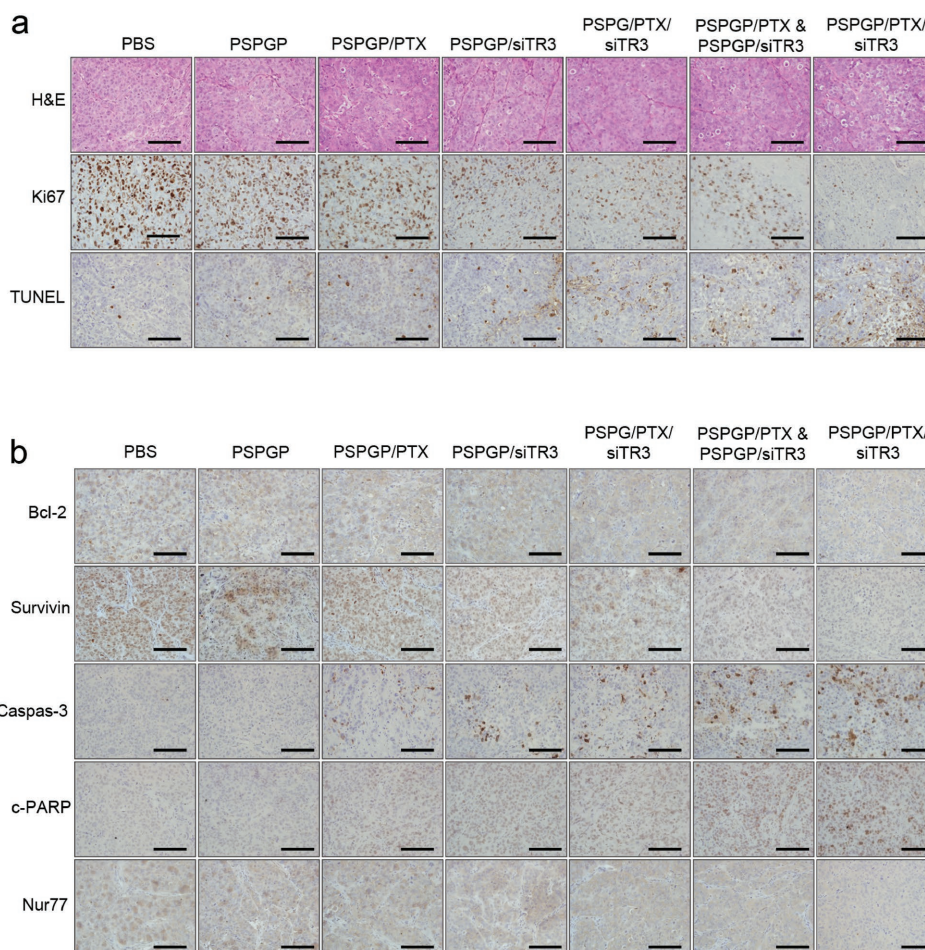


Figure 8. a) H&E, Ki67, TUNEL and b) Nur77, Bcl-2, Survivin, c-Caspase, c-PARP immunohistochemistry analysis of tumor tissues of murine tumor models with Panc-1 xenografts after treatment with PBS, **PSPGP**, **PSPGP/PTX**, **PSPGP/siTR3**, **PSPGP/PTX/siTR3**, **PSPGP/PTX & PSPGP/siTR3**, and **PSPGP/PTX/siTR3**. The scale bars represent 40 μm .

PSPGP could be a potential strategy for targeted pancreatic cancer therapy.

Supporting Information

Supporting Information is available from the Wiley Online Library or from the author.

Acknowledgements

Y.L. and H.W. contributed equally to this work. This research was funded by the National Basic Research Program of China (Grant No. 2014CB931900). Animal care and handling procedures were in agreement with the guidelines evaluated and approved by the ethics committee of Zhejiang University. Study protocols involving animals were approved by the Zhejiang University Animal Care and Use Committee.

- [1] R. Siegel, J. Ma, Z. Zou, A. Jemal, *CA Cancer J. Clin.* **2014**, *64*, 9.
- [2] T. Conroy, J. Bachet, A. Ayav, F. Huguot, A. Lambert, C. Caramella, R. Maréchal, J. Van Laethem, M. Ducreux, *Eur. J. Cancer* **2016**, *57*, 10.
- [3] A. Gerritsen, M. Jacobs, I. Henselmans, J. van Hattum, F. Efficace, G. Creemers, I. H. de Hingh, M. Koopman, I. Q. Molenaar, H. W. Wilmink, O. R. Busch, M. G. Besselink, H. W. van Laarhoven, *Eur. J. Cancer* **2016**, *57*, 68.
- [4] X. Guo, Z. Cui, *Pancreas* **2005**, *31*, 13.
- [5] D. Cunningham, I. Chau, D. D. Stocken, J. W. Valle, D. Smith, W. Steward, P. G. Harper, J. Dunn, C. Tudur-Smith, J. West, S. Falk, A. Crellin, F. Adab, J. Thompson, P. Leonard, J. Ostrowski, M. Eatock, W. Scheithauer, R. Herrmann, J. P. Neoptolemos, *J. Clin. Oncol.* **2009**, *27*, 5513.
- [6] J. P. Neoptolemos, J. A. Dunn, D. D. Stocken, J. Almond, K. Link, H. Beger, C. Bassi, M. Falconi, P. Pederzoli, C. Dervenis, L. Fernandez-Cruz, F. Lacaine, A. Pap, D. Spooner, D. J. Kerr, H. Friess, M. W. Büchler, *Lancet* **2001**, *358*, 1576.
- [7] X. Deng, M. Cao, J. Zhang, K. Hu, Z. Yin, Z. Zhou, X. Xiao, Y. Yang, W. Sheng, Y. Wu, Y. Zeng, *Biomaterials* **2014**, *35*, 4333.
- [8] X. Xiong, A. Lavasanifar, *ACS Nano* **2011**, *5*, 5202.
- [9] D. Lane, *Nat. Biotechnol.* **2006**, *24*, 163.
- [10] P. Huang, D. Wang, Y. Su, W. Huang, Y. Zhou, D. Cui, X. Zhu, D. Yan, *J. Am. Chem. Soc.* **2014**, *136*, 11748.
- [11] F. Li, X. Zhao, H. Wang, R. Zhao, T. Ji, H. Ren, G. J. Anderson, G. Nie, J. Hao, *Adv. Funct. Mater.* **2015**, *25*, 788.

- [12] B. Li, Q. Tang, D. Cheng, C. Qin, F. Y. Xie, Q. Wei, J. Xu, Y. Liu, B. Zheng, M. C. Woodle, N. Zhong, P. Y. Lu, *Nat. Med.* **2005**, *11*, 944.
- [13] Y. Zhang, C. Yang, W. Wang, J. Liu, Q. Liu, F. Huang, L. Chu, H. Gao, C. Li, D. Kong, Q. Liu, J. Liu, *Sci. Rep.* **2016**, *6*, 21225.
- [14] D. M. Dykxhoorn, C. D. Novina, P. A. Sharp, *Nat. Rev. Mol. Cell Biol.* **2003**, *4*, 457.
- [15] H. Shen, T. Sun, M. Ferrari, *Cancer Gene Ther.* **2012**, *19*, 367.
- [16] J. E. Zuckerman, M. E. Davis, *Nat. Rev. Drug Discovery* **2015**, *14*, 843.
- [17] M. E. Davis, J. E. Zuckerman, C. H. J. Choi, D. Seligson, A. Tolcher, C. A. Alabi, Y. Yen, J. D. Heidel, A. Ribas, *Nature* **2010**, *464*, 1067.
- [18] S. C. Semple, A. Akinc, J. Chen, A. P. Sandhu, B. L. Mui, C. K. Cho, D. W. Y. Sah, D. Stebbing, E. J. Crosley, E. Yaworski, I. M. Hafez, J. R. Dorkin, J. Qin, K. Lam, K. G. Rajeev, K. F. Wong, L. B. Jeffs, L. Nechev, M. L. Eisenhardt, M. Jayaraman, M. Kazem, M. A. Maier, M. Srinivasulu, M. J. Weinstein, Q. Chen, R. Alvarez, S. A. Barros, S. De, S. K. Klimuk, T. Borland, V. Kosovrasti, W. L. Cantley, Y. K. Tam, M. Manoharan, M. A. Ciufolini, M. A. Tracy, A. de Fougères, I. MacLachlan, P. R. Cullis, T. D. Madden, M. J. Hope, *Nat. Biotechnol.* **2010**, *28*, 172.
- [19] C. Zheng, M. Zheng, P. Gong, J. Deng, H. Yi, P. Zhang, Y. Zhang, P. Liu, Y. Ma, L. Cai, *Biomaterials* **2013**, *34*, 3431.
- [20] N. Vinayavekhin, A. Saghatelian, *J. Am. Chem. Soc.* **2011**, *133*, 17168.
- [21] S. O. Lee, M. Abdelrahim, K. Yoon, S. Chintharlapalli, S. Papineni, K. Kim, H. Wang, S. Safe, *Cancer Res.* **2010**, *70*, 6824.
- [22] R. H. Stauber, W. Mann, S. K. Knauer, *Cancer Res.* **2007**, *67*, 5999.
- [23] S. D. Cho, K. Yoon, S. Chintharlapalli, M. Abdelrahim, P. Lei, S. Hamilton, S. Khan, S. K. Ramaiah, S. Safe, *Cancer Res.* **2007**, *67*, 674.
- [24] W. Chen, Y. Yuan, D. Cheng, J. Chen, L. Wang, X. Shuai, *Small* **2014**, *10*, 2678.
- [25] T. Yin, L. Wang, L. Yin, J. Zhou, M. Huo, *Biomaterials* **2015**, *61*, 10.
- [26] R. Kanasty, J. R. Dorkin, A. Vegas, D. Anderson, *Nat. Mater.* **2013**, *12*, 967.
- [27] X. Zhao, F. Li, Y. Li, H. Wang, H. Ren, J. Chen, G. Nie, J. Hao, *Biomaterials* **2015**, *46*, 13.
- [28] C. Zhu, S. Jung, S. Luo, F. Meng, X. Zhu, T. G. Park, Z. Zhong, *Biomaterials* **2010**, *31*, 2408.
- [29] C. W. Beh, W. Y. Seow, Y. Wang, Y. Zhang, Z. Y. Ong, P. L. R. Ee, Y. Yang, *Biomacromolecules* **2009**, *10*, 41.
- [30] Z. Xu, Z. Zhang, Y. Chen, L. Chen, L. Lin, Y. Li, *Biomaterials* **2010**, *31*, 916.
- [31] H. Meng, M. Liong, T. Xia, Z. Li, Z. Ji, J. I. Zink, A. E. Nel, *ACS Nano* **2010**, *4*, 4539.
- [32] A. M. Chen, M. Zhang, D. Wei, D. Stueber, O. Taratula, T. Minko, H. He, *Small* **2009**, *5*, 2673.
- [33] S. Biswas, P. P. Deshpande, G. Navarro, N. S. Dodwadkar, V. P. Torchilin, *Biomaterials* **2013**, *34*, 1289.
- [34] Z. J. Deng, S. W. Morton, E. Ben-Akiva, E. C. Dreaden, K. E. Shopsowitz, P. T. Hammond, *ACS Nano* **2013**, *7*, 9571.
- [35] S. Shi, K. Shi, L. Tan, Y. Qu, G. Shen, B. Chu, S. Zhang, X. Su, X. Li, Y. Wei, Z. Qian, *Biomaterials* **2014**, *35*, 4536.
- [36] T. Yin, P. Wang, J. Li, Y. Wang, B. Zheng, R. Zheng, D. Cheng, X. Shuai, *Biomaterials* **2014**, *35*, 5932.
- [37] X. Zhang, Z. Zhang, X. Xu, Y. Li, Y. Li, Y. Jian, Z. Gu, *Angew. Chem. Int. Ed.* **2015**, *54*, 4289.
- [38] Z. Zhang, X. Zhang, X. Xu, Y. Li, Y. Li, D. Zhong, Y. He, Z. Gu, *Adv. Funct. Mater.* **2015**, *25*, 5250.
- [39] K. Wang, Q. Hu, W. Zhu, M. Zhao, Y. Ping, G. Tang, *Adv. Funct. Mater.* **2015**, *25*, 3380.
- [40] K. A. Kelly, N. Bardeesy, R. Anbazhagan, S. Gurumurthy, J. Berger, *PLoS Med.* **2008**, *4*, 657.
- [41] Y. Ping, Q. Hu, G. Tang, J. Li, *Biomaterials* **2013**, *34*, 6482.
- [42] Y. Ping, C. Liu, Z. Zhang, K. L. Liu, J. Chen, J. Li, *Biomaterials* **2011**, *32*, 8328.
- [43] D. Peer, J. M. Karp, S. Hong, O. C. Farokhzad, R. Margalit, R. Langer, *Nat. Nanotechnol.* **2007**, *2*, 751.
- [44] M. C. Williams, *Proc. Natl. Acad. Sci. USA* **1984**, *81*, 6054.
- [45] S. Tang, Q. Yin, J. Su, H. Sun, Q. Meng, Y. Chen, L. Chen, Y. Huang, W. Gu, M. Xu, H. Yu, Z. Zhang, Y. Li, *Biomaterials* **2015**, *48*, 1.
- [46] L. Han, C. Tang, C. Yin, *Biomaterials* **2015**, *60*, 42.
- [47] T. Sun, J. Du, Y. Yao, C. Mao, S. Dou, S. Huang, P. Zhang, K. W. Leong, E. Song, J. Wang, *ACS Nano* **2011**, *5*, 1483.
- [48] S. K. Kolluri, X. Zhu, X. Zhou, B. Lin, Y. Chen, *Cancer Cell* **2008**, *19*, 367.

Received: August 14, 2016
Published online: October 20, 2016